Available online at www.sciencedirect.com
ScienceDirect
Journal of Photochemistry and Photobiology A: Chemistry 194 (2008) 37–48
Journal of Photochemistry and Photobiology A:Chemistry
www.elsevier.com/locate/jphotochem

# 1-(2-Quinolyl)-2-naphthol: A new intra-intermolecular photoacid–photobase molecule

T.C. Chien [a,*], L.G. Dias [d], G.M. Arantes [a], L.G.C. Santos [a], E.R. Triboni [b], E.L. Bastos [c], M.J. Politi [b,*]

[a] *Departamento de Química Fundamental, Instituto de Química, Universidade de São Paulo, P.O. Box 26077, São Paulo SP 005513-970, Brazil*
[b] *Laboratório Interdepartamental de Cinética Rápida, Departamento de Bioquímica, Instituto de Química, Universidade de São Paulo, P.O. Box 26077, São Paulo SP 005513-970, Brazil*
[c] *Centro de Ciências Naturais e Humanas, Fundação Universidade Federal do ABC, Rua Santa Adélia, 166, 09210-170 Santo André, SP, Brazil*
[d] *Departamento de Química, Faculdade de Filosofia Ciências e Letras de Ribeirão Preto, Universidade de São Paulo, 14040-901 Ribeirão Preto, SP, Brasil*

Received 19 March 2007; received in revised form 10 July 2007; accepted 16 July 2007
Available online 22 July 2007

**Abstract**

Photochemical and photophysical properties of 1-(2-quinolyl)-2-naphthol (2QN) in water and organic solvents, as well in glassy media were studied to investigate the occurrence of intramolecular excited state prototropic reactions between the naphthol and quinoline rings. Spectral data show the two chromophores apparently behaving independently. However, in acid aqueous media or in low polarity solvents a new electronic transition red shifted band with respect to that of the parent compounds assigned to an intramolecular H-bond and to a quinoid form, respectively, shows up. Model calculations and R–X data lend support to a minimum energy conformer having a dihedral angle of $\sim 39^{\circ}$ between the two groups. Singlet excited state properties ($S_1$) show a high suppressive effect of one ring over the other, resulting in very low emission yields at room temperature. The occurrence of excited state intramolecular proton transfer is observed in water (zwitter ion form) and in low polarity media (quinoid form) and originates from a previously CT H-bonded state. Phosphorescence data allowed a reasonable description of the electronic states of 2QN. In addition two new derivatives were prepared having the N atom blocked by methylation and both the N and O groups blocked by a $CH_2$ bridge. The spectral data of these two compounds confirmed the attributions made for 2QN.


*Keywords:* Photoacid; Photobase; Charge transfer; Excited state intramolecular proton transfer

## 1. Introduction

Proton transfer reactions are of utmost relevance in chemistry and biochemistry [1,2]. Ground and excited state proton transfer reactions play a fundamental role in several systems like enzymes and proteins [3,4]. Intermolecular and intramolecular proton transfer [5] are important mechanistic tools for the study of a great deal of processes and structures, like lateral proton conduction in proteins [6], environmental probes in micelles [7,8], reversed micelles [9,10], pH jump [11,12], cyclodextrins [13,14], lipid bilayers [15], photolithography [16], films [17] and so far.

Photoacids and photobases [18–20] denote molecules that present a change in the excited state $pK_a$ ($pK_a^*$) when prototropic reactions are competitive with the excited state (usually singlets) deactivation pathways. The change in the acidity and basicity in the excited state is ascribed to the promotion of the electron to an isoelectronic state where the new electronic configuration changes the bond strengths for the acid and basic groups.

In this study the photochemical and photophysical characterization of 1-(2-quinolyl)-2-naphthol (2QN) are presented (Scheme 1). This compound was originally synthesized as an anti-malarial drug [21] and to the best of our knowledge no photochemical or photophysical studies were done. From a spectroscopist viewpoint 2QN is a quite special compound since it

* Corresponding authors at: Av. Prof. Lineu Prestes, 748 Bloco 12 Superior, Sala 1258, 05508-900 São Paulo, SP, Brazil. Tel.: +55 11 3091 3877; fax: +55 11 3091 3877.
*E-mail addresses:* chienusp@yahoo.com.tw (T.C. Chien), mjpoliti@usp.br (M.J. Politi).

1010-6030/$ – see front matter © 2007 Elsevier B.V. All rights reserved.
doi:10.1016/j.jphotochem.2007.07.012

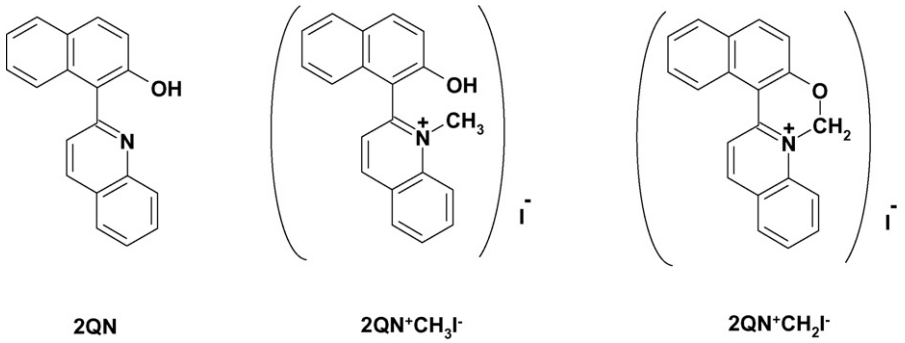


Scheme 1. Chemical structures of 1-(2-quinolyl)-2-naphthol (2QN), 1[2-(*N*-methyl)-quinolinium]-2-naphthol ($2QNCH_3^+I^-$) and the *N*,2-[(1-oxa)-ethane]-1-(2-quinolinium)-naphthalene ($2QNCH_2^+I^-$).

enclosures two chromophoric groups (naphthol and quinoline) having opposite acid base properties. Naphthol [22,23] and quinoline [18,24,25] are well-known compounds due to their singlet excited state intermolecular photoacid and photobase properties, respectively. The relevant issue here investigated is to establish if the intermolecular process can be expressed into an intramolecular one. In certain aspect 2QN can be viewed as an extension of more common hydroxyquinolines [26,27] or 10-hydroxybenzo[*h*]quinoline [28,29].

The experimental approach included the preparation and characterization of the title compound added to the photophysical and photophysical determinations. Furthermore, the preparation and spectral studies of two new compounds, namely the 1[2-(*N*-methyl)-quinolinium]-2-naphthol ($2QNCH_3^+I^-$) and the *N*,2-[(1-oxa)-ethane]-1-(2-quinolinium)-naphthalene ($2QNCH_2^+I^-$) to confirm the spectral behavior (Scheme 1) are included.

It will be shown that a minimum energy conformer of 2QN is a twisted molecule due to the sterical hindrance between the two rings leading to a dihedral angle of ∼39°. Fluorescence yields of the several species of 2QN are very low at room temperature in the solvents investigated indicating deactivation by vibrational motions. The observation of fluorescence emission from the quinoid isomer in aprotic media and of the naphtholate in protic media shows the occurrence of excited state prototropic reactions.

## 2. Materials and methods

### 2.1. Materials

#### 2.1.1. 1-(2-Quinolyl)-2-naphthol (2QN)

1-(2-Quinolyl)-2-naphthol (2QN) (Scheme 1). 2QN was synthesized by the condensation reaction between *o*-aminobenzaldeheyde (0.3 g) and 1-acetyl-2-naphthol (0.4 g, Aldrich) in absolute ethanol (12 mL) with an aliquot of 4 mL of sodium ethoxide (prepared by adding sodium in absolute ethanol) [30,31]. After 2–3 h reflux, 2QN was precipitated with $HCl_{(aq)}$. Orange crystals were obtained: yield, 81%; mp: 138–140 °C, anal. ($C_{19}H_{13}NO$) found: C 84.3%, H 4.86%, N 5.36%; $^1$H NMR ($CDCl_3$, 300 MHz) $\delta$ 7.31 (d, $J$ = 8.91 Hz, 1H), $\delta$ 7.36 (ddd, $J$ = 8.00, 6.95, 1.12 Hz, 1H), $\delta$ 7.48 (ddd, $J$ = 8.46, 6.89, 1.43 Hz, 1H), $\delta$ 7.60 (ddd, $J$ = 8.07, 6.99, 1.14 Hz, 1H), $\delta$ 7.78 (ddd, $J$ = 8.43, 6.97, 1.41 Hz, 1H), $\delta$ 7.853 (d, $J$ = 9.32 Hz, 1H), $\delta$ 7.84 (d, $J$ = 9.32 Hz, 1H), $\delta$ 7.88 (dd, $J$ = 8.18, 0.99 Hz, 1H), $\delta$ 8.05 (d, $J$ = 8.74 Hz, 1H), $\delta$ 8.11 (d, $J$ = 8.35 Hz, 1H), $\delta$ 8.23 (d, $J$ = 8.32 Hz, 1H), $\delta$ 8.29 (d, $J$ = 8.68 Hz, 1H), $\delta$ 13.35 (s(broad), 1H).

#### 2.1.2. o-Aminobenzaldeheyde

*o*-Aminobenzaldeheyde [32] was obtained by the reduction of *o*-nitrobenzaldeheyde (Aldrich). The reaction mixture contained *o*-nitrobenzaldeheyde (1.2 g), Iron(II) sulfate heptahydrate (21.0 g, Aldrich), distilled water (35 mL) and concentrated hydrochloric acid (0.1 mL, Aldrich). The mixture was heated to a temperature of ∼90 °C. Then 5 mL of concentrated ammonium hydroxide ($NH_4OH$) was added, following two minutes interval three 6 mL portions of ammonium hydroxide were added. After 30 min of reaction, the product was collected by steam distillation. The compound was obtained as colorless crystals from chilled saturated with NaCl water: yield ∼75%. The compound was used shortly after its preparation.

#### 2.1.3. 1[2-(N-Methyl)-quinolinium]-2-naphthol iodide

1[2-(*N*-Methyl)-quinolinium]-2-naphthol iodide ($2QNCH_3^+I^-$) (Scheme 1). This new compound was prepared by mixing 2QN (0.027 g) and iodomethane $CH_3I$ (0.6 mL, Aldrich) in acetonitrile (5 mL, Merck) at room temperature. After ∼15 days $2QN^+CH_3I^-$ orange crystals were obtained: yield ∼100% mp: 265–268 °C; $^1$H NMR ($CDCl_3$, 300 MHz) $\delta$ 7.30–7.36 (m, 1H), $\delta$ 7.42–7.52 (m, 3H), $\delta$ 7.99–8.45 (m, 1H), $\delta$ 8.11 (d, $J$ = 7.50 Hz, 1H), $\delta$ 8.17 (d, $J$ = 8.70 Hz, 2H), $\delta$ 8.34 (ddd, $J$ = 8.85, 7.20, 1.50 Hz, 1H), $\delta$ 8.57 (d, $J$ = 8.10 Hz, 1H), $\delta$ 8.66 (d, $J$ = 9.00 Hz, 1H), $\delta$ 9.31 (d, $J$ = 8.40 Hz, 1H), $\delta$ 11.11 (s, 1H).

#### 2.1.4. N,2-[(1-Oxa)-ethane]-1-(2-quinolinium)-naphthalene ($2QNCH_2^+I^-$)

*N*,2-[(1-Oxa)-ethane]-1-(2-quinolinium)-naphthalene ($2QNCH_2^+I^-$) (Scheme 1). The $2QNCH_2^+I^-$, also a new compound, was prepared by dissolving 2QN (0.1 g) in acetonitrile in the presence of NaOH (0.02 g) and adding di-iodomethane (50 μL, Aldrich) and let at room temperature for ∼15 days. Fol-

lowing the product was separated by circular chromatography (Chromatotron) using acetone:hexane 2:5 (v:v) as the eluent. Yield (15%). MS *m/z* (relative intensity) 127.15 (11, $I^-$), 270.20 (100), 284.20 (20, $M^+$); $^1$H NMR ($CDCl_3$, 300 MHz) $\delta$ 6.89 (s, 2H), $\delta$ 7.42 (d, $J$ = 9.0 Hz, 1H), $\delta$ 7.67 (m, 1H), $\delta$ 7.86 (m, 1H), $\delta$ 7.94 (m, 1H), $\delta$ 8.01 (d, $J$ = 8.10 Hz, 1H), $\delta$ 8.23 (d, $J$ = 9.00 Hz, 1H), $\delta$ 8.27 (m, 1H), $\delta$ 8.53 (d, $J$ = 9.00 Hz, 1H), $\delta$ 8.58 (d, $J$ = 8.70 Hz, 1H), $\delta$ 8.68 (d, $J$ = 9.30 Hz, 1H), $\delta$ 8.95 (d, $J$ = 9.30 Hz, 1H).

2-Naphthol and quinoline were purchased from Aldrich, and purified by sublimation and recrystallization from ethanol, respectively. All other reagents were of the best available grade. All solutions were made with twice-distilled water and further purified by a Milli-Q system. Spectroscopic grade solvents were used in the spectroscopic determinations.

The ultraviolet/visible spectra were obtained in a Hitachi U2000 spectrophotometer, interfaced with a 386Sx PC computer using 1 cm quartz cuvettes except when noted. A Spex Fluorolog DM3000F spectrofluorometer having a phosphorimeter attachment was used for the fluorescence and phosphorescence emission and excitation recordings with right angle arrangement except when noticed. The spectra, in the ratio mode, were corrected using the correction files provided by SPEX. Solvent Raman scattering were recorded for each experiment and subtracted from that of the sample with the use of a built-in SPEX software, except for the spectrum of 2QN in hexane once the very low emission yield lead to deformation of the spectrum. Luminescence and phosphorecence experiments in glassy media EPA (ethylether, isopentane, ethanol, 5:5:1, v:v:v) and EP (ethyelther, isopentane, 1:1, v:v) were done using a liquid nitrogen bath in a transparent Dewar flask arranged inside the sample compartment of the spectrofluorometer, with the sample contained in a quartz cylindrical tube (0.5 cm internal diameter) inside the bath. All other experiments unless otherwise stated, were conducted at room temperature (~20 °C).

Photolysis experiments were done with an immersion lamp (Hannovia Hg low pressure $\lambda_{exc.}$ = 254 nm). The reaction vessel contained [2QN] ~$10^{-2}$ M in 25 mL ethanol for about 100 h (corresponding to ~10% of photoconversion to the main product) in an inert atmosphere (bubbling $N_2$). The reaction was followed by TLC and after the products were separated by a circular chromatography (Chromatotron model 7924T).

NMR spectra were recorded in a 300 or 500 MHz Bruker. pH measurements were done using a ORION (model 370) or a SENTRON (model 2001) pHmeters, using sure flow glass combination electrode (Orion) and a Ion sensitive field effect transistor probe (Sentron). pH's values were adjusted using when appropriate $HClO_4$, acetic acid and sodium acetate, $KH_2PO_4$ and $K_2HPO_4$, $Na_2B_4O_7$, $H_3BO_3$ and NaOH solutions from best grade available stock materials. Buffer concentrations were kept at ~20 mM.

X-ray determinations were done with a Enraf-Nonius (model CAD-4 Mach3). Softwares used to solve the structure were: SHELXS86 [33]; to refine the structure SHELXL97 [34]; and molecular graphics ZORTEP [35].

### 2.2. Methods

#### 2.2.1. Theoretical models

Ab initio calculations were performed to probe the conformational energetics of 2QN in its different protonation states. Gas-phase geometries of the conformers were fully optimized by the analytic gradient method at the restricted Hartree-Fock (RHF) level of theory using the standard 6-31G* basis set. Only real frequencies were found in vibrational frequency calculations of the conformational minima at the same theory level. The only two free dihedrals angles in 2QN and $2QNH^+$ (the torsion of the carbon–carbon bond between the two rings and the oxygen–carbon bond in the naphthol ring) and the only free dihedral angle in $2QN^-$ (the torsion of the carbon–carbon bond between the two rings) were scanned in a rigid potential energy surface (PES) search at the same level of theory. All ab initio calculations were performed with the Gaussian program [36].

Structures of 2QM, $2QM_{ZW}$ and $2QM_Q$ (see Scheme 2) were optimized without any constraints using the RM1 semiempirical method, as implemented in MOPAC2007 [37]. Geometry optimization and vertical excitation energies calculations were performed using the multi-electron configuration interaction (MECI) approach and the RM1 method, hereafter called RM1-CI. The active space was constructed with five molecular orbitals (MOs) and two double filled levels (C.I. = (5,2), 100 configurations in active space). Solvent effects on the optical properties were modeled using the conductor-like screening model (COSMO) [38].

#### 2.2.2. Optical absorption spectra

The conformational minima (42° and 313°, respectively) found for the neutral 2QN and protonated $2QNH^+$ were used for fixed geometries single-point calculations in vacuum using the INDO/S-CIS semi-empirical method [39] implemented in the GEOMOP program [40,41] in order to determine vertical transition energies and oscillator strengths. All singly excited configurations with energy less than two times the lowest excited configuration were used in the INDO/S-CIS calculations. Since we are not using doubly excited configurations, it is unnecessary to include single excitation with energy larger than double the lowest singly (doubly) excited energy.

## 3. Results and discussion

Structures of 2QN and of two new derivatives are presented in Scheme 1. The structures are drawn in a way to depict the spatial proximity between the –OH photoacid and the aromatic –N photobase groups. Notice that upon methylation of 2QN, leading to ions $2QNCH_3^+$ and $2QNCH_2^+$, the acid and base groups are reduced to the naphtholic OH in $2QNCH_3^+$ and none in the $2QNCH_2^+$, respectively.

### 3.1. Electronic spectra

The UV–vis spectra of 2QN in aqueous media as function of pH are presented in Fig. 1((A) acid and (B) basic media, respectively). The transition from the monoprotonated (quinolinium

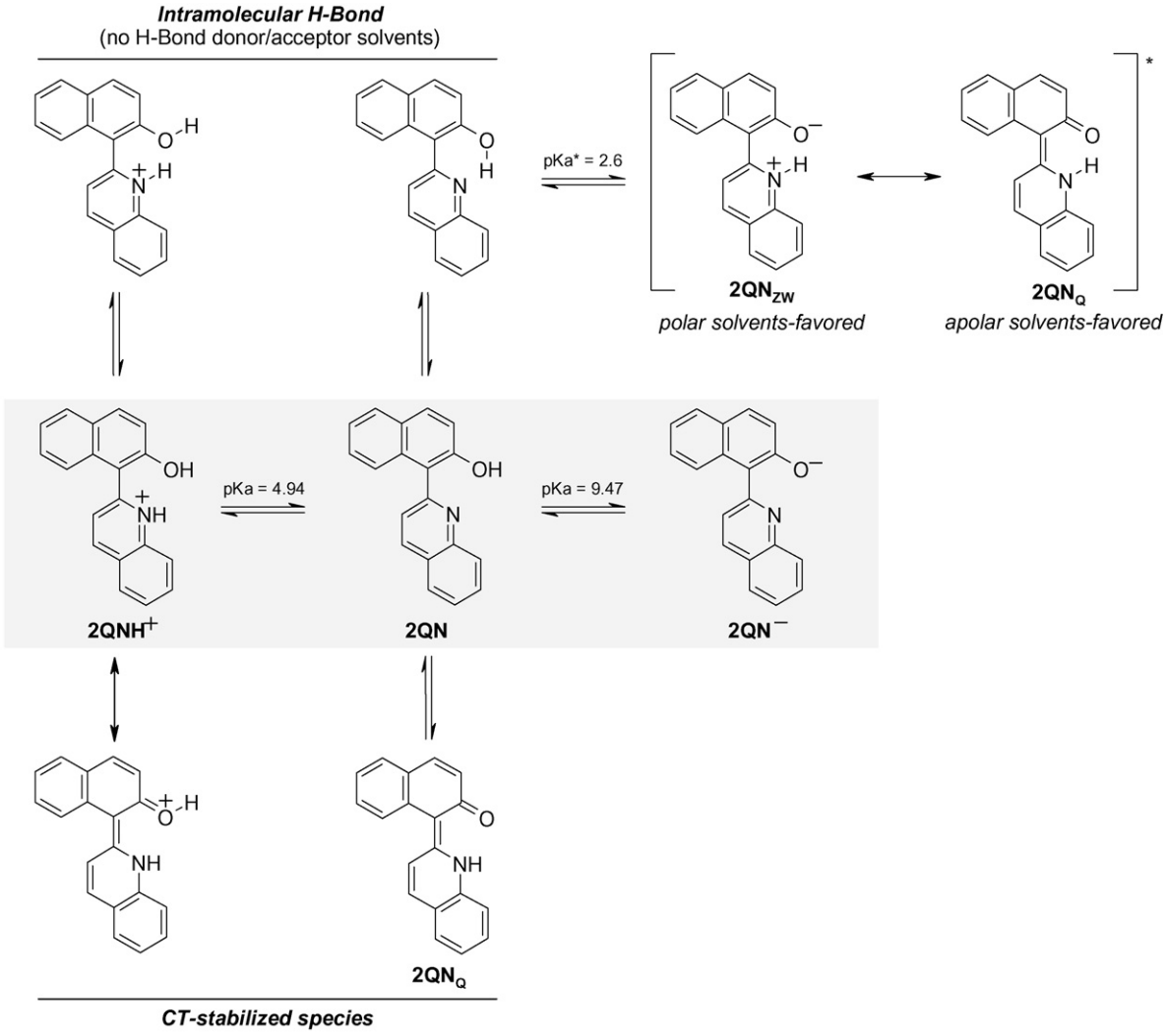


Scheme 2. Representation of pH, solvent and electronic effects on 2QN.

moiety), to the neutral (quinolylnaphthol) and to the monoanion (naphtholate residue) species as function of pH can be easily observed. A clear isosbestic point is observed at ~343 nm. In acidic media two main electronic transitions are observed at ~312 and 388 nm. In basic conditions, main transitions appear at 275, 312 and 360 nm (transitions below 240 nm were not analyzed). Also, from the data in Fig. 1, p$K_a$s determinations are straightforward. The p$K_a$ values of 4.55 and 9.30 for the quinoline and 2-naphthol moieties, respectively, are close to the values of the parent compounds (4.94 for quinoline [19,42] and 9.47 for 2-naphthol [19]) and show the electron withdrawing effect of one ring over the other, that is, the effect of the quinoline ring as a substituent in the 2-naphthol ring, and vice versa.

These spectra apparently resemble that of the sum of the individual contributions of quinoline and naphthol groups. Accordingly, comparing the UV–vis spectrum of a mixture of quinoline and 2-naphthol at various pH and at approximately the same concentration as that of 2QN, reveals the spectral independence of the two chromophoric rings in 2QN, except for the transition at 388 nm in acidic condition (Fig. 2 and Table 1). In other words, the electronic transitions due to naphthol and to quinoline moieties appear isolated or just summing up in the spectra of 2QN. Moreover, changing the pH, the spectral response can be assigned to the titration of the individual rings. Thus, increasing the pH the naphtholate (2QN$^{-}$) absorption spectra shows up, as well by decreasing the pH the absorption of the quinolinium (2QNH$^{+}$) moiety appears. This explanation is also consistent when the molar absorptivities ($\varepsilon$) shown in Table 1 are considered. Taking, for example, the $\varepsilon$ at 277 nm for 2QN at pH 7 which is ~7200 $M^{-1}$ $cm^{-1}$, it can be decomposed in the contributions due to the quinoline ring ($\varepsilon$ = 3600 $M^{-1}$ $cm^{-1}$) plus that of the naphthol group ($\varepsilon$ = 4200 $M^{-1}$ $cm^{-1}$). It should be noticed, however, that absorption bands from 2QN are overall broader than those of the individual compounds as should be expected for a larger and supposedly more solvated as well having more vibrational modes molecule.

The transition peaking at 388 nm in acid condition is assigned to the protonated quinoline ring. The large shift in the absorption wavelength maximum ($\lambda_{max}$) compared with that of pure quinolinium ($\lambda_{max}$ = 310 nm) would be ascribed to a stabilization effect caused by hydrogen bonding and/or charge

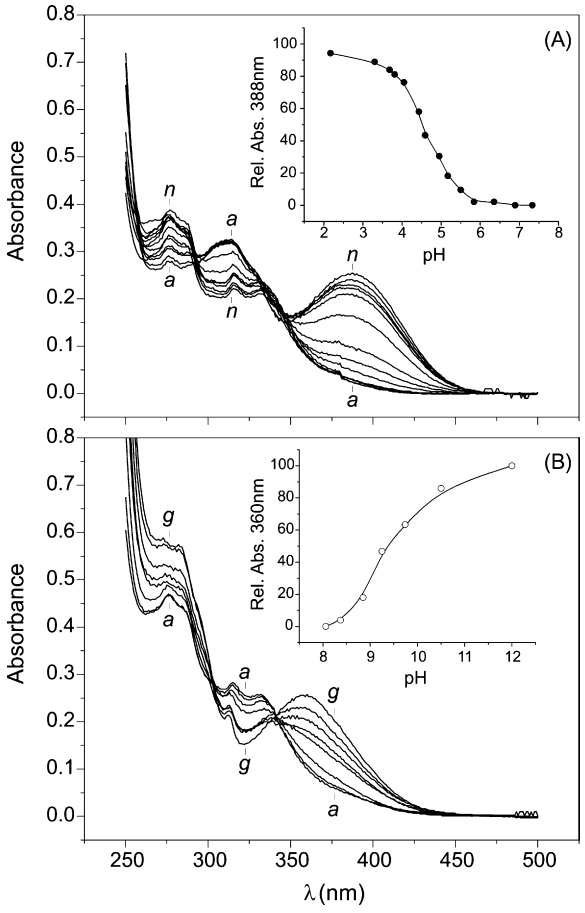


Fig. 1. (A) UV–vis absorption spectra of 2QN in water, from (a to n), pH 2.17; 3.30; 3.68; 3.81; 4.05; 4.43; 4.59; 4.95; 5.17; 5.50; 5.84; 6.35; 6.89; 7.33, respectively. (Inset) Relative absorbance at 388 nm vs. pH. (B) Same as (A) but in alkaline media, from (a to g), pH 8.06; 8.37; 8.85; 9.26; 9.74; 10.5; ~12, respectively. (Inset) Relative absorbance at 360 nm vs. pH. ([2QN] = $10^{-5}$ M, with 5 cm pathlength quartz cuvette, room temperature).

transfer (CT) involving the naphthol OH group and the aromatic nitrogen in the quinoline ring. A similar effect is also observed in the absorbance spectra of 2QN in organic media (Fig. 3). Going from neutral aqueous solution to MeOH, EtOH, $CH_3CN$ and hexane the transition peaking around 380 nm shows up.

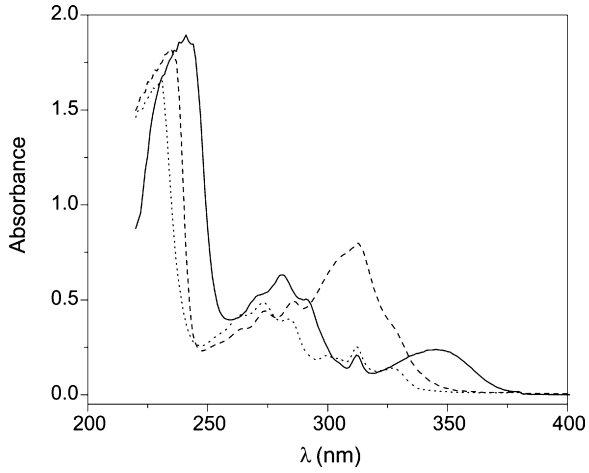


Fig. 2. UV–vis absorption spectra of aqueous solutions of quinoline ([Q] = 1.51 × $10^{-4}$ M) and 2-naphthol ([N] 1.35 × $10^{-4}$ M) at pH's 1 (—) (0.1 M $HClO_4$), 7 (. . .) ($H_2O$) and 14 (– – –) (1 M NaOH).

In Scheme 2 the various 2QN, $2QNH^+$ and $2QN^-$ species according to the solvent property (polarity and proticity), pH and p$K_a$s, are depicted. Starting with an aqueous neutral solution (2QN), change in pH results in the formation of $2QNH^+$ in acidic media (Fig. 1A and inset) and of $2QN^-$ in alkaline conditions (Fig. 1B and inset).

For 2QN in the presence of polar H-bond donor/acceptor solvents, both hydroxyl naphtholic group and quinoline moiety are solvated and the chromophores behave independently. In less polar and less H-bond-effective solvents, stabilization can be achieved through $H^+$ shift/CT (from naphthol to quinoline) with the concomitant formation of a quinoid structure ($2QN_Q$), favoring electron delocalization (see Scheme 2). From $2QNH^+$, CT would also occur, leading to a cationic quinoid species, whose delocalization results in bathochromic band shift. One should notice that both structures are similar except by the protonation of the naphtholic hydroxyl group. The formation of a quinoid species in the electronic excited state is also possible through

Table 1
Values of $\lambda_{abs}^{max}$, $\varepsilon^{max}$ and p$K_a$ of 2-naphthol, quinoline and 2QN in $H_2O$ at three pH's

| Compound | Medium | $\lambda_{abs}^{max}$ (nm) | $\varepsilon^{max}$ ($M^{-1}$ $cm^{-1}$) | Compound[a] | Medium | $\lambda_{abs}^{max}$ (nm) | $\varepsilon^{max}$ ($M^{-1}$ $cm^{-1}$)[b] |
|---|---|---|---|---|---|---|---|
| | | 280 | 8740 | | | 245 | 59000 |
| $2QN^-$ | $H_2O$ (pH 12) | 312 | 7360 | 2-Naphtholate ($N^-$) | $H_2O$ (pH 12) | 280 | 6500 |
| | | 360 | 5160 | | | 348 | 3000 |
| | | 277 | 7200 | | | 230 | 36000 |
| | | | | Quinoline (Q) | $H_2O$ (pH 12) | 275 | 3600 |
| | | 312 | 5520 | | | 312 | 4500 |
| 2QN | $H_2O$ (pH 7–8) | | | | | 230 | 57000 |
| | | 335 | 2890 | 2-Naphthol (N) | $H_2O$ (pH ~2) | 275 | 4200 |
| | | | | | | 325 | 2100 |
| | | 276 | 5800 | | | 238 | 37500 |
| $2QNH^+$ | $H_2O$ (pH ~2) | 312 | 6900 | Quinolinium ($QH^+$) | $H_2O$ (pH ~2) | | |
| | | 388 | 5360 | | | 312 | 7100 |

[a] Ewing, G.W., Steck, E.A., Absorption spectra of heterocyclic compounds. I. Quinolinols and isoquinolinols. Journal of the American Chemical Society 68 (1946) 2181–7.

[b] The values of $\varepsilon^{max}$ are means.

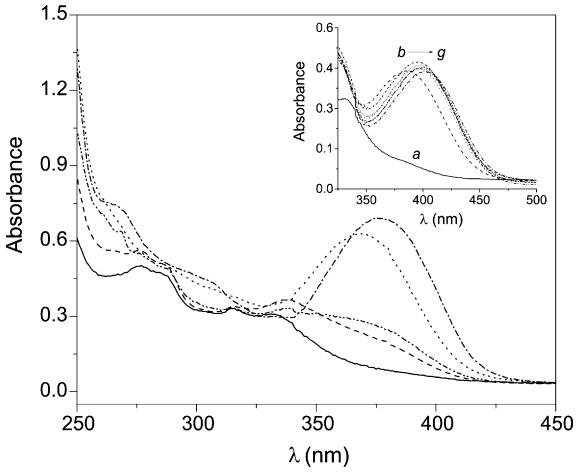


Fig. 3. UV–vis absorption spectra of 2QN in (—) $H_2O$, (– – –) MeOH, (–·–·–) EtOH, (. . .) ACN and (–·–·–) hexane. (Inset) UV–vis absorbance spectra of 2QN in $H_2O$ (a), 0.1 M aqueous $HClO_4$ (b) and with varying amounts of EtOH (containing 0.1 M $HClO_4$) from (c to f) (35, 37.5, 64.3, 100%, v:v, EtOH:$H_2O$) ([2QN] = $5 \times 10^{-5}$ M).

$H^+$ shift from the excited intramolecular H-bond 2QN in apolar solvents. In polar solvents, formation of the zwitterionic form ($2QN_{ZW}$) should be favored.

In H-bonding media, as in water and in low molecular weight alcohols, H-bond of N and OH groups of 2QN with the solvent is dominant. This effect can be further demonstrated by analysing the spectra shown in Fig. 3 inset. In this experiment the effect of EtOH in the absorption spectra of $2QNH^+$ is shown. The addition of a lower dielectric constant protic solvent to the system red shifts the absorption maximum as a consequence of decreasing the energy gap for the electronic transition (Table 1). The apparently large $\varepsilon$ arises from the transition being from on ring to the other, that is, from an appropriate geometry between the two rings. A plausible explanation is that the non-bonded electron ($n$) from the naphthol oxygen finds an "overlapped" $\pi^*$ of the quinoline ring giving rise to a favorable transition. This finding will be further discussed with the model calculations and photochemical data presented below.

Charge transfer from the oxygen lone pair (naphthol) to the positively charged quinolinium nitrogen (aqueous acidic media) or to the unprotonated quinoline nitrogen (2QN) increases the bond order between the rings (C1–C2) and will bring the dihedral angle between the rings to a quasi planar conformation, increasing conjugation. However, one must consider that a complete planar structure (i.e., dihedral angle ~0°) is not plausible, mainly due to the interaction between hydrogen atoms in quinoline and naphthol groups. In order to further investigate the dependence of the structural and electronic parameters on solvent effects we have performed geometry optimization and bond order computations of 2QN and $2QN_{ZW}$ using the RM1 method [43]. Geometry optimization of the first singlet excited state was performed using the multi-electron configuration interaction (MECI) approach and the RM1 method. The effect of solvents of varying dielectric constant on structures and energies of the probes was assessed using the conductor-like screening model (COSMO), i.e., water, acetonitrile, methanol, ethanol, dichloromethane, hexane and

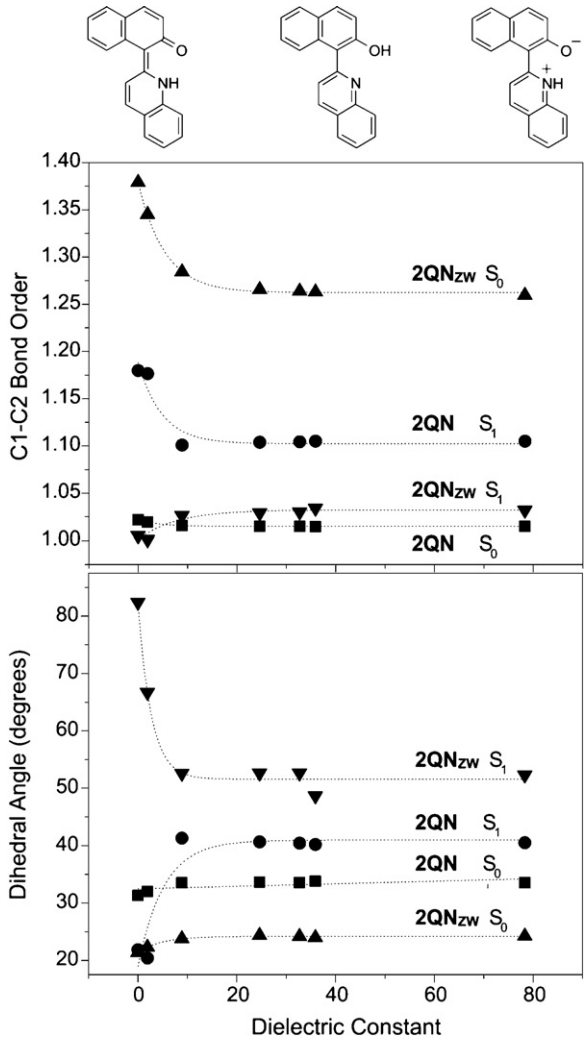


Fig. 4. Singlet ground and excited state C1–C2 bond order and central dihedral angle for 2QN and $2QN_{ZW}$ calculated in vacuum and in several polarizable continua parameterized with dielectric constants equivalent to water, acetonitrile, methanol, ethanol, dichloromethane and hexane.

compared with that calculated in vacuum. Results are presented in Fig. 4.

Both, C1–C2 bond order and dihedral angle of 2QN shows no dependence on the dielectric constant of the solvent. This indicates that solvent polarity show little or no effect on the geometry of 2QN. However, it must be pointed out that polarizable continuum approach does not explicitly consider specific solute/solvent interactions, e.g., H-bonds. For $2QN_{ZW}$, i.e., after $H^+$ shift, the dihedral angle (~20°) is not significant affected by medium polarity, but C1–C2 bond order increases as the dielectric constant decreases. In this way, it is reasonable to consider that rings in the ground state of 2QN are free to rotate, whereas in $2QN_{ZW}$ they are not. These results corroborate with the $H^+$ shift/CT approach.

At the first singlet excited state, C1–C2 bond orders are slightly increased when compared with the ground state. In low polarity solvents, the $S_1$ state of 2QN shows a quinoid character and consequently low dihedral angles. As the polarity increases, charge densities in OH and N are stabilized, reduc-

ing intramolecular hydrogen bond strength and consequently increasing the dihedral angle. This result would indicate that CT occurs through hydrogen bond, but further theoretical analysis would be performed in order to confirm this hypothesis [44]. Proton transfer in excited state is thus favored in low polarity solvents and results in $2QN_{ZW}$ in $S_1$ state. In low dielectric constant solvents, proton transfer should be followed by rotation of rings (C1–C2) and thus OH···N hydrogen bond is no longer possible. Briefly, 2QN shows intramolecular CT in excited state as solvent polarity decreases, whereas the same effect is observed for $2QN_{ZW}$ in ground state. These effects are more evident in solvents with $\varepsilon$ lower than 10. Furthermore, the observed solvatochromism, the large extinction coefficients, the lack of vibrational resolution in the ~388 nm band and also the changes in $pK_a$ from the isolated compounds to the diad show that the quinoline protonates with more difficulty in 2QN and the naphthol deprotonates more easily in 2QN, i.e., confirms an electron withdrawing effect from the quinoline to the naphthol or, in other words, a charge transfer from the naphthol to the quinoline. These results are compatible with charge transfer mechanism observed in solvatochromic probes and 6-hydroxyquinoline and indicate that CT would be favored by $H^+$ shift [45].

### 3.2. Model calculations and crystal structure

#### 3.2.1. Conformational energy

Ab initio calculations were performed to probe the conformational energetics of 2QN in its different protonation states. Gas-phase geometries of the conformers were fully optimized by the analytic gradient method at the restricted Hartree-Fock (RHF) level of theory using the standard 6-31G* basis set. Only real frequencies were found in vibrational frequency calculations of the conformational minima at the same theory level. The only two free dihedrals angles in 2QN and $2QNH^+$ (the torsion of the carbon–carbon bond between the two rings and the oxygen–carbon bond in the naphthol ring) and the only free dihedral angle in $2QN^-$ (the torsion of the carbon–carbon bond between the two rings) were scanned in a rigid potential energy surface (PES) search at the same level of theory.

Fig. 5A shows the relative energy for the conformers in 2QN with different protonation states. The zero of energy for each curve corresponds to the most stable conformer and the dihedral angle between the rings is defined as the dihedral C(naphthol)–C(naphthol)–C(quinoline)–C(quinoline). For neutral 2QN, the global minimum, i.e., the most stable conformer, is located at 42° of the dihedral angle between the two rings. There is another stable minimum at 282° which is 5.7 kcal $mol^{-1}$ more energetic. The barriers for the conformational inter-conversion are around 25 kcal $mol^{-1}$, from the most stable to the second minimum, and around 33 kcal $mol^{-1}$, from the second minimum to the most stable one (regarding the direction of increasing dihedral angle value). The torsion of the oxygen–carbon bond in the naphthol ring (data not shown) results in structures consistently higher in energy except around dihedral angle 160°. In this region, near the barrier between the two minima, the smaller

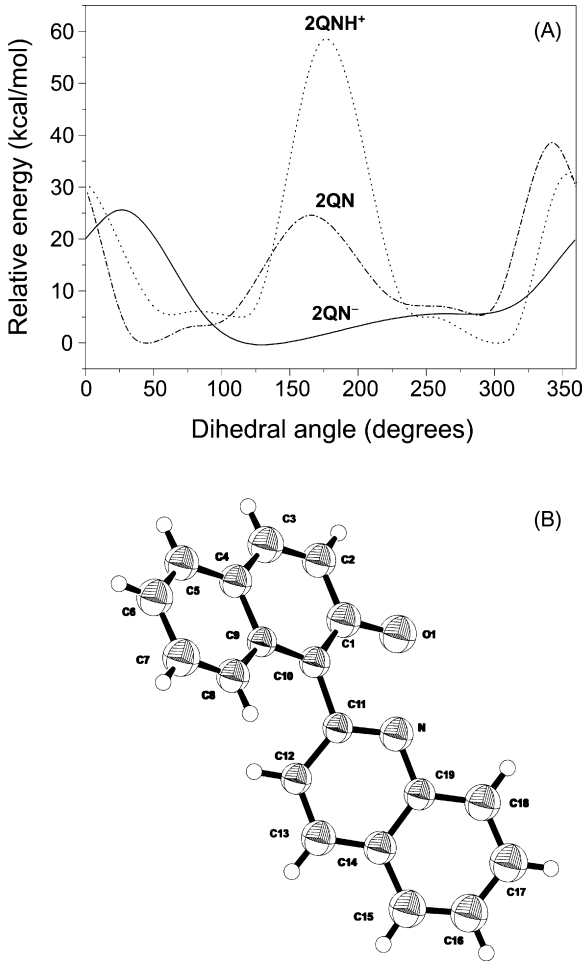


Fig. 5. (A) Calculated conformational energy and (B) crystal structure of 2QN.

energy structure found with torsion of the oxygen–carbon bond is 5.4 kcal $mol^{-1}$ smaller than the energy shown in Fig. 5A for the 2QN.

For the protonated $2QNH^+$, there are also two minima and the global minimum is located at 305° of the dihedral angle. The second minimum has 5.0 kcal $mol^{-1}$ more energy and is located at 112°. However, there are barriers of around 32 and 58 kcal $mol^{-1}$ separating the two minima. The torsion of the oxygen–carbon bond in the naphthol ring results in a partial PES consistently higher in energy (data not shown).

The ionized $2QN^-$ has only one minimum at 145° and a barrier for the carbon–carbon torsion of 26 kcal $mol^{-1}$. It should be noted that the barrier heights presented are good estimations from the rigid PES scans, but no transition state geometry was optimized.

#### 3.2.2. Crystal structure

X-ray diffraction of 2QN leads to the structure depicted in Fig. 4. The dihedral angle found is ~39° in close agreement with that calculated. The distance between the C–C bond joining the two rings is 1.49 Å characteristic of a typical σ bond. Furthermore, the hydrogen atom from the OH group could not be observed pointing its high mobility. This observation is also in agreement with the H NMR data for this atom which shows

a broad band with a chemical shift in $CDCl_3$ of ~13.3 ppm (see Section 2.1).

### 3.3. Optical absorption spectra

The INDO/S-CIS calculation in vacuum resulted in two absorption lines in wavelengths higher than 250 nm and with oscillator strengths higher than 0.07 for the 2QN and $2QNH^+$ minima conformers. For 2QN there is one transition line in 321 nm (oscillator strength 0.21), with major contribution (CI exponent −0.7311) of an excitation from the highest occupied molecular orbital (HOMO) to the second lowest unoccupied molecular orbital (LUMO + 1). There is another absorption line for 2QN in 296 nm (oscillator strength 0.31), with major contribution (CI exponent −0.7012) of an excitation from the highest occupied molecular orbital (HOMO) to the lowest unoccupied molecular orbital (LUMO).

For $2QNH^+$ there is one transition line in 396 nm (oscillator strength 0.18), with major contribution (CI exponent −0.9176) of an excitation from the highest occupied molecular orbital (HOMO) to the lowest unoccupied molecular orbital (LUMO). There is another absorption line in 317 nm (oscillator strength 0.21), with major contribution (CI exponent 0.7724) of an excitation from the highest occupied molecular orbital (HOMO) to the second lowest unoccupied molecular orbital (LUMO + 1).

A Mülliken population analysis for both the ground and excited state electronic densities was performed and the difference between the atomic charges summed upon the two different rings for each state was computed. For 2QN, the first transition (321 nm, HOMO → LUMO + 1) present a small depletion of 0.07e (electron charge) in the naphthol ring and a resultant appearance of the same amount of charge in the quinoline ring. The second excitation (296 nm, HOMO → LUMO) has a small appearance of 0.21e in the naphthol ring. For $2QNH^+$, the first transition (396 nm, HOMO → LUMO) present a large depletion of 0.82e in the naphthol ring and the second excitation (317 nm, HOMO → LUMO + 1) has a considerable depletion of 0.61e in the naphthol ring.

The HOMO → LUMO + 1 excitation around 320 nm is clearly conserved between the two protonation states of 2QN. For the protonated cation $2QNH^+$ there is an exchange in the order of the excitations. The HOMO → LUMO transition at 396 nm results in a large relocation of charge between the rings and hence a large dipole change.

These findings corroborate the experimental data and reinforce the assignment of a CT transition of high $\varepsilon$ for the electronic transition of $2QNH^+$ at ~390 nm as depicted in Scheme 2 (Fig. 1 and Table 1).

### 3.4. Fluorescence emission

Normalized fluorescence emission spectra of 2QN species in aqueous media are presented in Fig. 6. Emission wavelength maxima ($\lambda_{em}^{max}$) going from alkaline to acid condition appear at 409, 439 and 490 nm, respectively. These transitions can be attributed to the naphtholate ring (409 nm emission), from the quinolinium via intramolecular $H^+$-transfer (439 nm emission),

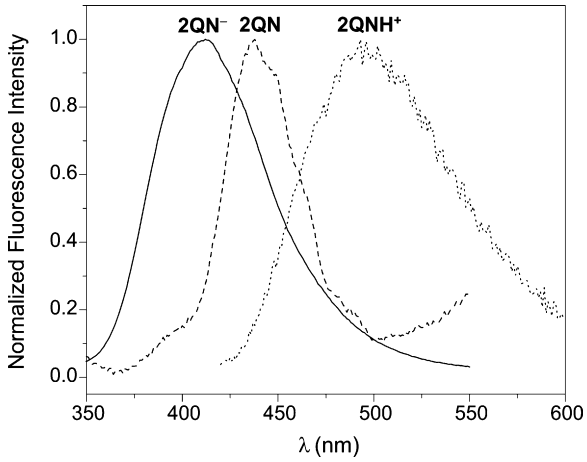


Fig. 6. Normalized corrected fluorescence emission spectra of 2QN at pH's 1 (—) (0.1 M $HClO_4$), 7 (– – –) ($H_2O$) and 12 (. . .) (0.01 M NaOH) (conditions: slits exc. = 1/1 mm, emi. = 2/2 mm, $\lambda_{exc.}$ = 304 nm, [2QN] = $10^{-5}$ M).

and from the quinolinium via ground-state protonated quinoline $2QNH^+$ (490 nm emission), respectively. These assignments are made in comparison with the pure compounds (Table 2), for the transitions at 409 and 439 nm. It should be notice, however, the very small quantum yields of 2QN species compared with that of the parent compounds. The decrease in fluorescence yields is ascribed to the presence of a neighbor aromatic group that by vibrational motion increases the internal conversion deactivation pathway. In other words, when the excitation is on the naphthol ring the close by quinoline acts as a quencher, and vice versa. Albeit the fluorescence yields are very low, the emissions at ~400 nm (shoulder) and 439 nm (main) shows the occurrence of intramolecular $H^+$-transfer from neutral 2QN, that is from the naphthol (photoacid) moiety to the quinoline (photobase) (see Scheme 2). Furthermore, it suggests the study of the fluorescence behavior at low temperatures or in rigid media (see below). The emission at 490 nm assigned to the $2QNH^+$ shows the contribution of the naphthol ring (O–H bonded to the quinolinium ring) in decreasing the energy gap for the transition.

Emission spectra data of 2QN in organic media are summarized in Table 2 and Fig. 7. Typically only one unstructured

Table 2
Values of $\lambda_{em}^{max}$ and $\phi_{flu}$ of 2QN, 2-naphthol and quinoline in $H_2O$, MeOH, EtOH, $CH_3CN$ and hexane

| Compounds | Medium | $\lambda_{em}^{max}$ (nm) | $\phi_{flu}$ |
|---|---|---|---|
| | $H_2O$ (pH 1) | 490 | 0.0011 |
| | $H_2O$ (pH ~7) | 439 | 0.0035 |
| | $H_2O$ (pH 12) | 409 | 0.0120 |
| 2QN | MeOH | 422 | 0.0025 |
| | EtOH | 418 | 0.0038 |
| | $CH_3CN$ | 415 | 0.0019 |
| | Hexane | 414 | <0.001 |
| Naphthol | $H_2O$ (pH 1) | 352 | 0.2 |
| Naphtholate | $H_2O$ (pH 12) | 416 | 0.26 |
| Quinoline | $H_2O$ (pH 1) | 384 | 0.05 |
| Quinolinium | $H_2O$ (pH 12) | 440 | 0.06 |

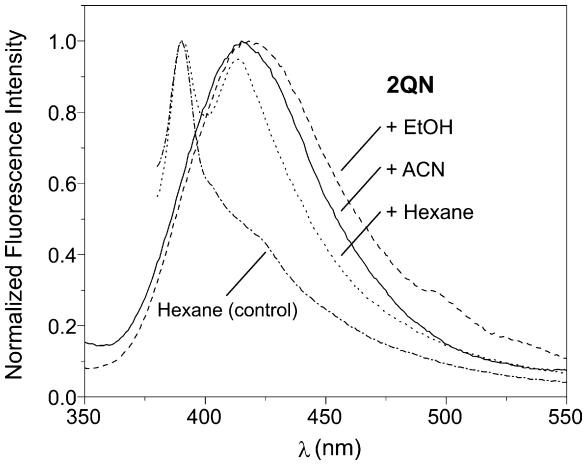


Fig. 7. Normalized corrected fluorescence emission spectra of 2QN in organic solvents (—) EtOH, (– – –) ACN and (. . .) hexane (conditions as in Fig. 6).

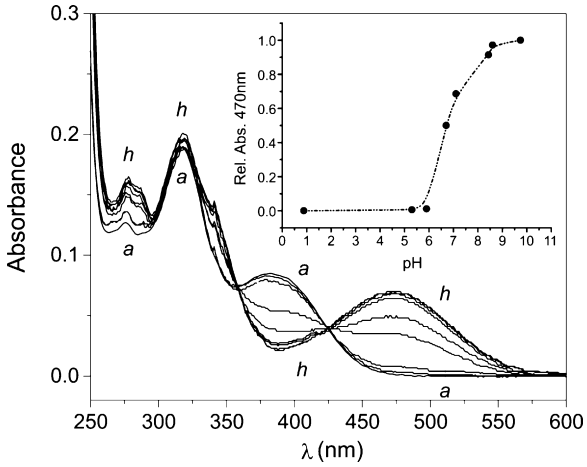


Fig. 8. UV–vis absorption spectra of $2QNCH_3^+$ from (a to h), pH 0.88, 5.30, 5.90, 6.70, 7.10, 8.43, 8.60 and 9.74, respectively. (Inset) Relative absorbance at 470 nm vs. pH. ($[2QNCH_3^+] = 2.42 \times 10^{-5}$ M).

emission peaking at ~415 nm shows up. This band is assigned to the emission derived from the quinoid form (see Scheme 2). Considering the isolated chromophores, the fluorescence yields of naphthol and naphtholate are higher than those of quinoline species (Table 2). Thus, if these relative yields are kept in 2QN, the other expected emission from the quinolinium ring will be very small. Raman spectra of hexane is included in the figure to show the low emission yield of 2QN (see 2QN spectrum in hexane). It should be considered however that the overall fluorescence yield of 2QN are very low and for a more detailed description further determinations are necessary (Table 2). A small blue shift in the emission maxima going from ethanol, acetonitrile and hexane of ~3 nm, consistent with a CT transition is observed (Table 2). An interesting aspect is the appearance of a small shoulder in the spectra in ethanol at ~500 nm. This will be shown below to be due to a photochemical reaction.

### 3.5. Properties of 2QN derivatives

In order to better understand the spectral behavior of 2QN, the properties of two new derivatives were determined (Scheme 1). Fig. 8 depicts the spectra of $2QNCH_3^+I^-$ in water as a function of pH. The transition at 320 nm does not vary with pH and is, therefore, assigned to the *N*-methyl-quinolinium band whereas the bands at 466 and 388 nm change with pH in accordance with an acid base reaction over the 2-naphthol moiety. Clearly the band at 388 nm is due to the undissociated group and that at 466 nm due to the 2-naphtholate. The $\varepsilon$'s for these transitions are 2890 and 3840 $M^{-1}\,cm^{-1}$, respectively. Also clear isosbestic points are seen at 425 nm and at 358 nm. From the titration curve a $pK_a$ of 6.70 is found, showing the effect of the positively charged quinolinium group compared with that of 2QN (Fig. 8 inset and Fig. 1B). Given the charge distribution it is likely that the neutral species dominates over the dipolar one (see Scheme 3). Molecular modelling is under way to explore this possibility.

In Fig. 9 the spectra of $2QNCH_2^+I^-$ is presented, a broad transition is observed peaking at 421 nm with a close by band

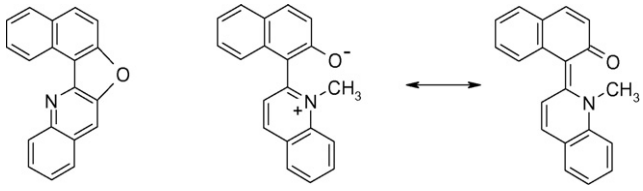

Scheme 3. Structure of photoproduct and conformations $2QN^+CH_3I^-$.

at 348 nm. The quite high $\varepsilon$ value for the band at 421 nm 18,110 $M^{-1}\,cm^{-1}$ points to an interaction between the two aromatic systems leading to a pseudo-planar form. However, like for $2QNCH_3^+I^-$ further studies with $2QNCH_2^+I^-$ are required to better establish its electronic states and minimum energy configurations. The emission spectrum of $2QNCH_2^+I^-$ which is independent of pH is quite simpler and presents only a main transition at 530 nm with an fluorescence yield of ~40% (Fig. 9). This emission yield is orders of magnitude higher than those of 2QN and $2QNCH_2^+I^-$ and points again to an interaction of the two aromatic systems.

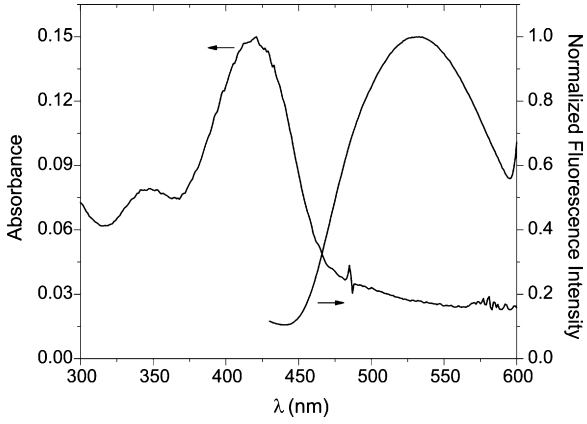


Fig. 9. Absorption and normalized corrected fluorescence emission spectra of $2QNCH_2^+$ ($[2QNCH_2^+] = 8.11 \times 10^{-6}$ M) at pH 7 ($H_2O$) (conditions: slits exc. = 1.5/1.5 mm, emi. = 3/3 mm, $\lambda_{exc.}$ = 305 nm).

### 3.6. Photochemistry of 2QN

A detailed study of the photochemistry of 2QN will be presented elsewhere. Here only the results from the photolysis of 2QN in ethanolic medium are presented (see Fig. 7). In Fig. 10 the emission spectra of 2QN as function of light exposition are presented. A small increase in the emission at ~420 nm is observed, along with the appearance of a structured emission peaking at 497, 533 and 573 nm. The main photoproduct obtained from a scaled up conditions (photolysis with an immersion Hg lamp and following the reaction by TLC) was isolated and from $^{13}C$ and $^{1}H$ NMR (DEPT, COSY and HETCOR), mass and FTIR the structure shown in Scheme 3 is found (data to be presented elsewhere). The proposed mechanism for the photoreaction is SN-aromatic derived from the rotation of the quinoline group relative to the naphthol. Such mechanism is in agreement with the attribution of 2QN emission spectra in ethanol or $H_2O$. In these solvents by H-bonding with the N atom from the quinoline and with the OH from the naphthol a rotamer having these groups in opposite sides is favored. The high fluorescence emission yield of the photoproduct is also in agreement with that observed for $2QNCH_2{}^+I^-$ which appear at the same spectral region. It should be pointed however that the structure in the photoproduct is likely to have the aromaticity spanned over the five rings. In Fig. 10 inset it is shown the effect of EtOH in promoting the photoreaction in a EP medium. Clearly the photoproduct starts to appear only after the addition of the protic solvent.

### 3.7. Glassy media

In order to further exploit the characteristics of 2QN emission it behavior in glassy matrix was investigated. Given the effect of ethanol in the photochemistry of 2QN at room temperature, two glassy matrix were assayed, first the well known EPA and a second one named EP (where the ethanol from EPA was removed, see Section 2). Although the gelation of the EP system lead to a somewhat opaque medium, spectra using the cylindrical cell and the Dewar filled with liquid $N_2$ could be collected. The spectra in these two media are almost the same and show the lack of photoreactions at liquid $N_2$ temperature. The spectra presented in Fig. 11 show the following features the characteristic 2-naphthol and quinolinium transitions at 382 and 438 nm, respectively, are detected, added to three new peaks at 497, 533 and 573 nm. In EPA by other hand transitions are seen at 417, 438 nm, (characteristic of 2-naphtholate and quinolinium) added to the three new ones at 497, 533 and 573 nm. It should be noticed the strong dependence of the naphtholate emission with the solvent as previously shown [46]. In both solvents the emission practically disappear with the increase in temperature, that is, above the glassy temperature emission is almost null. The appearance of a photoproduct of similar emission as that above presented could be visually detected. An interesting feature is observed by monitoring the emission in a EP solution (at room temperature) to where it was added 50 μL of ethanol.

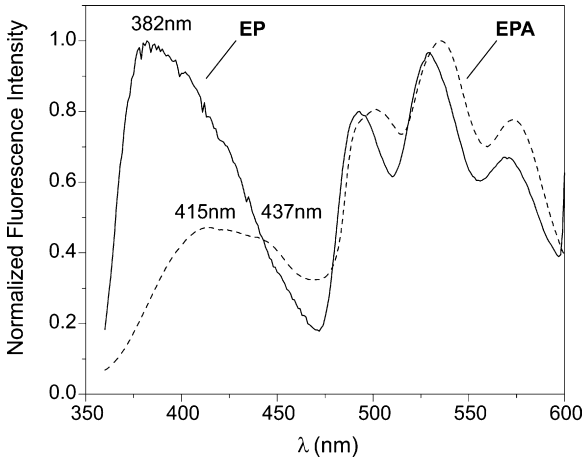


Fig. 11. Luminescence corrected emission spectra of 2QN in EPA and EP (conditions: temperature 77 K, slits exc. = 2/2 mm, emi. = 3/3 mm, $\lambda_{exc.}$ = 325 nm). ([2QN] = $10^{-5}$ M using 0.5 cm quartz cylindrical tube).

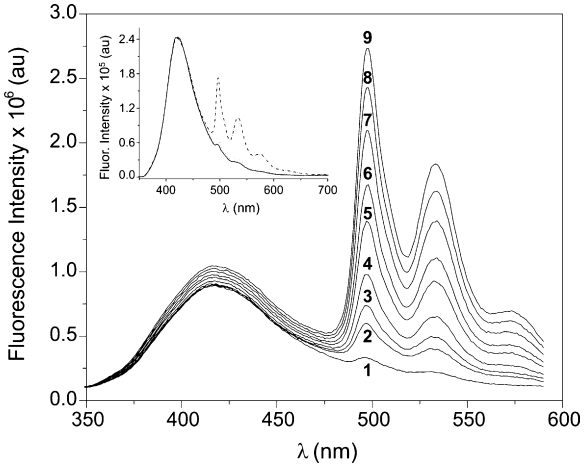


Fig. 10. Fluorescence emission spectra of 2QN in EtOH, from 1 to 9 every spectra ran about 2 min. (Inset) Fluorescence emission spectra after a little of EtOH (50 μL) added in 2QN's EP solution at room temperature (conditions: slits exc. = 1/1 mm, emi. = 2/2 mm, $\lambda_{exc.}$ = 304 nm, [2QN] = $10^{-5}$ M).

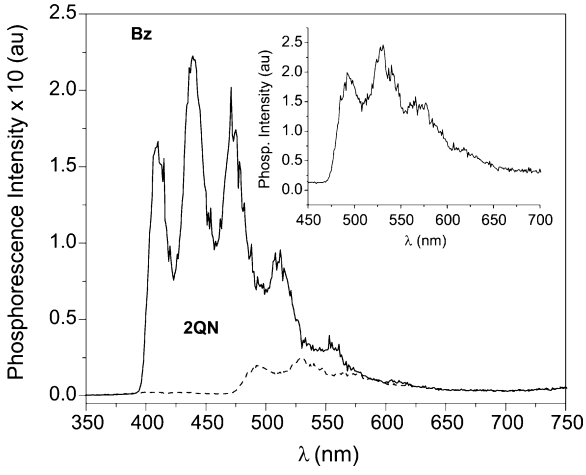


Fig. 12. Phosphorescence emission spectra of 2QN and of benzophenone (Bz) in EP (conditions: time delay = 0.04 ms, sample window = 100 ms, temperature 77 K, slits exc. = 3/3 mm, emi. = 3/3 mm, $\lambda_{exc.}$ = 260 nm). ([2QN] = [Bz] = $2 \times 10^{-5}$ M using 0.5 cm quartz cylindrical tube).

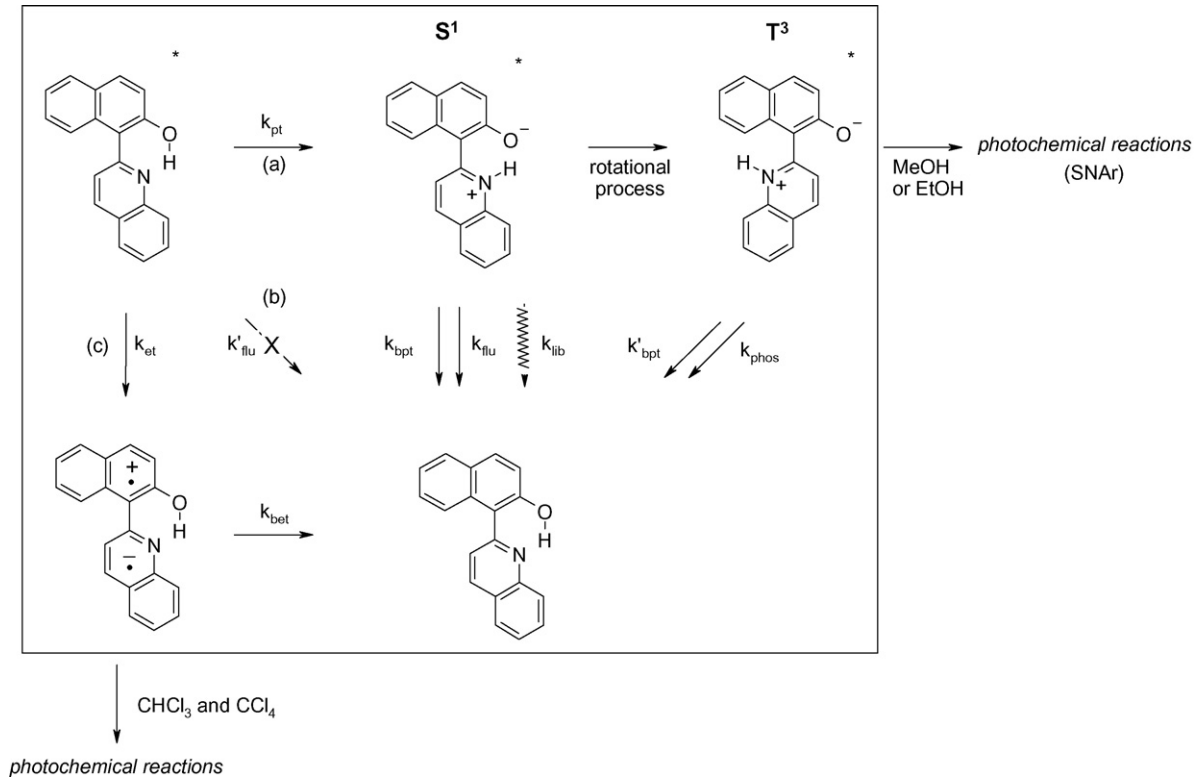


Scheme 4. Photochemical reaction pathways.

Clearly as noticed above a photoproduct evolves with time (Fig. 10 inset).

### 3.8. Phosphorescence spectra

The phosphorescence spectra of 2QN and of benzophenone, both in EPA, are presented in Fig. 12. Clearly a relatively high yield is found for 2QN (about 10 times smaller than that of benzophenone) triplet state, the phosphorescence emission shows a structured band peaking at 497, 533 and 573 nm as observed in the fluorescence emission spectra of the photolysis product of 2QN in ethanolic media suggesting a pseudo planar form with a extended interaction between the aromatic rings and furthermore a coupled proton transfer reaction. It must be added that no photoreactions were observed in the phosphorescence experiments.

Scheme 4 depicts the excited state reactions for 2QN. The following steps, as proposed by Tolbert and Nesselroth for 2-naphthol [22], are consistent with excitation being fixed at ~300 nm where both HOMO-LUMO + 1 and HOMO-LUMO transitions are likely to occur: (i) intramolecular transfer from the excited singlet 2QN (path a), followed by back proton transfer (bpt), fluorescence and internal conversion deactivations (flu,ic), and intersystem crossing to the triplet state (small angle rotation seems to take place), phosphorescence, photochemical reactions and so far; (ii) electron transfer from the quinoline to the naphthol ring, leading to the radical ions (path c), followed by back electron transfer (bet) and photochemical reactions. Certainly a more detailed investigation is necessary to the completeness of the reaction pathways.

## Acknowledgements

We wish to express our deep gratitude to the Brazilian funding agencies FAPESP (grants #98/02757-0 and #07/00684-6(E.L.B.)), CNPQ and CAPES. To Dr. A.C. Trindade for the work with X-ray determinations, to Mr. F.M. Oliveira and to Dr. I.A. Pérsio for the help with the NMR data collection and interpretation. This work is part of Dr. T.C. Chien Ph.D. Thesis work.

## References

[1] R.P. Bell, The Proton in Chemistry, second ed., Chapman Hall, London, 1973.
[2] E.F. Caldin, Proton-Transfer Reactions, Gold, fifth ed., Chapman Hall, London, 1975.
[3] P. Boyer, B. Chance, L. Ernster, P. Mitchell, E. Racker, E. Slater, Annu. Rev. Biochem. 46 (1977) 955–1026.
[4] H. Panefsky, J. Biol. Chem. 26 (1985) 13735–13741.
[5] L.G. Arnaut, S.J. Formosinho, J. Photochem. Photobiol. A: Chem. (1993), pp. 1–20 and 21–48.
[6] M. Gutman, Methods Biochem. Anal. 30 (1984) 1–103.
[7] M.J. Politi, H. Chaimovich, J. Phys. Chem. 90 (1986) 282–287.
[8] N. Chattopadhyay, R. Dutta, M. Chowdhury, J. Photochem. Photobiol. A: Chem. 47 (2) (1989) 249–257.
[9] M.J. Politi, O. Brandt, J.H. Fendler, J. Phys. Chem. 89 (11) (1985) 2345–2354.
[10] B. Cohen, D. Huppert, K.M. Solntsev, Y. Tsfadia, E. Nachliel, M. Gutman, J. Am. Chem. Soc. 124 (25) (2002) 7539–7547.
[11] J.H. Clark, S.L. Shapiro, A.J. Campillo, K.R. Winn, J. Am. Chem. Soc. 101 (5) (1979) 746–748.
[12] E. Nachiel, Z. Ophir, M. Gutman, J. Am. Chem. Soc. 109 (5) (1987) 1342–1345.

[13] A.U. Acuña, A. Costela, J.M. Muñoz, J. Phys. Chem. 90 (2) (1986) 2807–2808.
[14] N. Chattopadhyay, J. Photochem. Photobiol. A: Chem. 58 (1) (1991) 31–36.
[15] M. Gutman, E. Nachliel, Y. Tsfadia, in: E.A. Disalvo, S.A. Simon (Eds.), Permeability and Stability of Lipid Bilayers, CRC Press, Boca Raton, 1995, pp. 259–276.
[16] E.S. Mansueto, C.A. Wight, J. Am. Chem. Soc. 111 (5) (1989) 1900–1901.
[17] Y.V. Il'ichev, K.M. Solntsev, A.B. Demyashkevich, M.G. Kuz'min, H. Lemmetyinen, E. Vuorimaa, Chem. Phys. Lett. 193 (1992) 128–133.
[18] A. Weller, Z. Phys. Chem. 17 (1958) 224.
[19] J.F. Ireland, P.A.H. Wyattt, Adv. Phys. Org. Chem. 12 (1976) 131–221.
[20] S.G. Schulman, R.M. Threatte, A.C. Capomacchia, W.L. Paul, J. Pharm. Sci. 63 (1974) 876–880.
[21] W. Jenny, Helv. Chim. Acta 23 (61/62) (1954) 539–554.
[22] L.M. Tolbert, S.M. Nesselroth, J. Phys. Chem. 95 (25) (1991) 10331–10336.
[23] L.M. Tolbert, L.C. Harvey, R.C. Lum, J. Phys. Chem. 97 (50) (1993) 13335–13340.
[24] N. Mataga, Y. Kaifu, M. Koizumi, Bull. Chem. Soc. Jpn. 29 (1956) 373.
[25] C.A. Parker, Photoluminescence of Solutions, Elservier Publishing Company, Amsterdam, 1968, pp. 376 and 432.
[26] M. Itoh, T. Adachi, K. Tokumura, J. Am. Chem. Soc. 106 (4) (1984) 850–855.
[27] E. Bardez, A. Chatelain, B. Larrey, B. Valeur, J. Phys. Chem. 98 (9) (1994) 2357–2366.
[28] P.T. Chou, C.Y. Wei, J. Phys. Chem. 100 (42) (1996) 17059–17066.
[29] P.T. Chou, Y.C. Chen, W.S. Yu, Y.H. Chou, C.Y. Wei, Y.M. Cheng, J. Phys. Chem. A 105 (10) (2001) 1731–1740.
[30] M.Z.A. Badr, M.M. Alv, Tetrahedron 28 (1972) 3401–3406.
[31] G.O. Dudek, Spectrochim. Acta 19 (1963) 691–700.
[32] L.I. Smith, J.W. Opie, Org. Synth. 28 (1948) 11–13.
[33] G.M. Sheldrick, SHELXS86 Program for the Solution of Crystal Structures, University of Gottingen, Germany, 1990.
[34] G.M. Sheldrick, SHELXL97 Program for the Refinement of Crystal Structures, University of Gottingen, Germany, 1997.
[35] L. Zsolnai, ZORTEP: Na Interactive Molecular Graphics Program, University of Heidelberg, Germany, 1995.
[36] M.J. Frisch, et al., Gaussian 98 Rev. A.9, Gaussian Inc., Pittsburgh, PA, USA, 1998.
[37] J.J.P. Stewart, MOPAC2007, Stewart Computational Chemistry, 2007, Version 7.176W, http://www.OpenMOPAC.net.
[38] A. Klamt, G. Schüümann, COSMO: a new approach to dielectric screening in solvents with explicit expressions for the screening energy and its gradient, J. Chem. Soc., Perkin Trans. 2 (1993) 799.
[39] J.E. Ridley, M.C. Zerner, Theor. Chim. Acta 32 (1973) 111.
[40] D. Rinaldi, P.E. Hoggan, A. Cartier, K. Baka, G. Monard, M. Loos, A. Mokrane, V. Dillet, V. Thery, GEOMOSP: Semi-Empirical Computational Package, 2001. This soft is based on D. Rinaldi, P.E. Hoggan, A. Cartier, QCPE Bull., 1989.
[41] N. Reuter, M. Loos, G. Monard, A. Cartier, B. Maigret, J.L. Rivail, Mol. Eng. 7 (1997) 349–365.
[42] S.G. Schulman, A.C. Capomacchia, J. Am. Chem. Soc. 95 (9) (1973) 2763–2766.
[43] G.B. Rocha, R.O. Freire, A.M. Simas, J.J.P. Stewart, J. Comput. Chem. 27 (2006) 1101–1111.
[44] W.H. Thompson, J.T. Hynes, J. Am. Chem. Soc. 122 (2000) 6278–6286.
[45] (a) C. Reichardt, Solvents and Solvent Effects in Organic Chemistry, VCH, Weinheim, 2003;
(b) A. Abbotto, L. Beverina, S. Bradamante, A. Facchetti, C. Klein, G.A. Pagani, M. Redi-Abshiro, R. Wortmann, Chem. Eur. J. 9 (2003) 1991;
(c) E. Bardez, A. Chatelain, B. Larrey, B. Valeur, J. Phys. Chem. 98 (9) (1994) 2357–2366.
[46] J.P. Soumillion, P. Vandereecken, M. Van der Auweraer, F.C. De Schryver, A. Schanck, J. Am. Chem. Soc. 111 (6) (1989) 2217–2225.